Available online at www.sciencedirect.com
ScienceDirect
Journal of Power Sources 174 (2007) 877–882
JOURNAL OF POWER SOURCES
www.elsevier.com/locate/jpowsour

Short communication

Investigation of positive electrodes after cycle testing of high-power Li-ion battery cells IV An approach to the power fading mechanism by depth profile analysis of electrodes using glow discharge optical emission spectroscopy

Yoshiyasu Saito*, Md. Khalilur Rahman

Energy Technology Research Institute, National Institute of Advanced Industrial Science and Technology (AIST), AIST Tsukuba Central 2, 1-1-1 Umezono, Tsukuba, Ibaraki 305-8568, Japan

Available online 3 July 2007

Abstract

Depth profile of constituent elements of positive electrodes in lithium-ion batteries was analyzed by using glow discharge optical emission spectroscopy (GD-OES) from the surface to the interface with the current collector. Not only in pristine electrode but also in degraded electrode after 50,000 cycles of high rate charge and discharge, almost homogeneous concentration profile of lithium was observed, suggesting that particles of active electrode material in the deep region inside the electrode layer also concerned in the electrochemical reaction as well as the particles in the surface area. From observation of particles shape by scanning electron microscope (SEM), remarkable cracks were not observed in particles inside the electrode even in the degraded electrodes.

Keywords: Lithium-ion battery; Positive electrode; Degradation; Depth profile; Glow discharge optical emission spectroscopy (GD-OES)

1. Introduction

In recent years, lithium-ion batteries were widely used as power source for many kinds of portable electronic devices. In the next step of the technology, development of lithium-ion batteries with high-power characteristics are expected for applications to hybrid electric vehicles (HEV) and fuel cell hybrid electric vehicles (FCHV) as well as portable power tools. Long calendar life beyond 10 or 15 years is one of important requirements for such usage, especially in the power retention of the battery. It is indispensable to know the degradation mechanism of the battery for improvement of the calender life.

In our previous study [1], we focused the characterization of electrochemical side reactions occurring during charge and discharge of a lithium-ion battery, especially in high rate cycling, by calorimetric measurement. Excess heat generation caused by side reactions was detected, and correlated to enlargement of reaction resistance at the positive electrode after cycling. Some of the causes of power fading of the lithium-ion battery would be surface materials formed on the positive electrode by the side reactions resulting in the growth of reaction resistance. Recently several efforts are carried out to characterize the surface materials and structures by XANES [2], XPS [3], and FT-IR [4] and so on by our cooperative researchers, and these analyses are giving us some suggestive information. For example, on the positive electrode of the degraded batteries, some surface materials such as lithium carbonate and lithium alkyl carbonate have been formed as well as lithium deficient cubic phase has appeared in the active material. On the other hand, these results only reflect information of the most surface vicinity of the electrode. In fact, the thickness of the electrode is generally in several 10 or so micrometers. In addition, the electrode is not so dense but rather porous, and the electrolyte permeates into the clearance between the particles of the active material. Thus the electrode reaction does not proceed only at the surface of the electrode layer, and reaction inside the layer is not negligible. Although, since diffusion of lithium ions is not so fast both in the electrolyte and in the active material, large concentra-

* Corresponding author. Tel.: +81 29 861 5198; fax: +81 29 861 5799.
E-mail address: y-saito@aist.go.jp (Y. Saito).

0378-7753/$ – see front matter © 2007 Elsevier B.V. All rights reserved.
doi:10.1016/j.jpowsour.2007.06.223

tion gradient may be produced in the electrode during cycling. For instance, in the simulation study of Doyle et al. [5], large concentration gradient of lithium in a porous electrode layer in depth direction during high rate discharging was estimated. As a consequence, the question that whether the surface information represents whole electrode properties has to be considered. However, there are few reports to discuss about depth profile of the lithium inside the whole electrode.

Glow discharge optical emission spectroscopy (GD-OES) is an essential and convenient technique for the elemental surface analysis and depth profiling [6,7]. In this method, sample is placed as a cathode of the lamp, and sputtered from the surface by cathode sputtering phenomenon in glow discharge condition, and then optical emission of sputtered atoms in Ar plasma was analyzed by spectroscopy. Since the sputter progresses to deeper region of the sample with time, the result gives depth profile of constituent elements of the sample. With its high sputtering rates, GD-OES has been used generally for depth profiling of relatively thick film such as coatings of coated steels [8]. Recently, it is reported that GD-OES is also useful for analysis of thin film of which thickness is under 100 nm, and the depth resolution is comparable to secondary ion mass spectrometry [9,10]. In this study, GD-OES is applied to characterization of electrodes of lithium-ion battery to obtain depth profiles of the constituent elements from the surface to the interface with the current collector. Furthermore, for the positive electrodes of lithium-ion batteries degraded by cycling, depth profiles of constituent elements are analyzed and the relation between degradation of the batteries and depth profiles of the elements is discussed.

2. Experimental

In order to verify the accuracy of the GD-OES for electrode of the lithium-ion battery, $LiNi_{0.80}Co_{0.15}Al_{0.05}O_2$ was selected as the standard active material, and model cells using this material were assembled. In the preparation of the electrode, 86 wt% of the active material, 7 wt% of polyvinylidene fluoride (PVdF) binder, and 7 wt% of acetylene black as a conductive agent were mixed with *N*-methyl-2-pyrrolidone, pasted on a 20 μm thick Al foil as a current collector, and then dried. Cylindrical lithium-ion cells with 18 mm in diameter and 65 mm in length were assembled using the electrode mentioned above. The negative electrode was consisted of non-graphitizable carbon (hard carbon) with PVdF binder on Cu foil. The electrolyte was mixed solvent of ethylene carbonate (EC) and dimethyl carbonate (DMC) containing 1 M $LiPF_6$ where volume ratio of EC and DMC was 1:2. After several cycles, the state of charge (SOC) of the cells was set to 0%, 50%, or 100% by constant current discharge or charge of *C*/3 rate at 25 °C where *C* had been decided as the initial capacity, and then the positive electrodes were extracted from the cells for analysis. Cut off voltage during set up the SOC is 4.2 V and 2.5 V for SOC = 100% and 0%, respectively.

The lithium-ion batteries supplied for degradation test were same as described in the previous related reports [2–4], where the active material for the positive electrode was $LiNi_{0.73}Co_{0.17}Al_{0.10}O_2$. The detailed chemistry of the other materials, characterization methods of the battery performance such as dc resistance, and procedure of cycle test to degrade the batteries, were described elsewhere by Kobayashi et al. [2]. The cycle test was carried out in Central Research Institute of Electric Power Industry by Kihira et al. [11,12].

The positive electrodes extracted from the batteries were soaked in DMC to wash off the $LiPF_6$ from the electrode surface, and then dried under vacuum at room temperature more than 10 h. Subsequently, the sample electrodes were cut to dimensions of 10 mm × 10 mm for GD-OES measurement. Depth profile analysis was carried out by using Radio Frequency Glow Discharge Spectrometer, JY-5000RF (Jobin Yvon, Horiba) with the sample specimen placed in a holder that was made the cathode. The sample was sputtered in an argon atmosphere of 300–400 Pa by applying a radio frequency of 13.56 MHz at a power of 15–20 W. The diameter of sputtered craters was approximately 2 mm. Measured wavelengths (nm) of emission for the constituent materials of the sample were as follows: Li, 670.78; Ni, 341.48; Co, 345.31; Al, 396.15; C, 156.14; H, 121.57.

3. Results and discussion

Fig. 1 shows typical images of a pristine electrode containing $LiNi_{0.80}Co_{0.15}Al_{0.05}O_2$ observed by using a scanning electron microscopy (SEM). In the cross-sectional view (Fig. 1a), aluminum current collector can be seen in lower part, and the thickness of the electrode layer is confirmed to about 30 μm. The

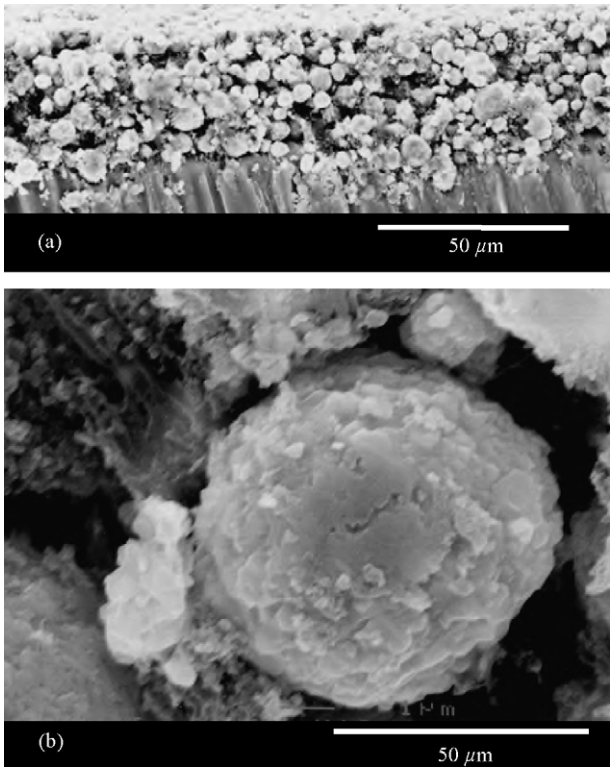

Fig. 1. SEM images of the standard positive electrode of a lithium-ion battery for GD-OES measurement: (a) cross-section view of the electrode and (b) particles of the active material.

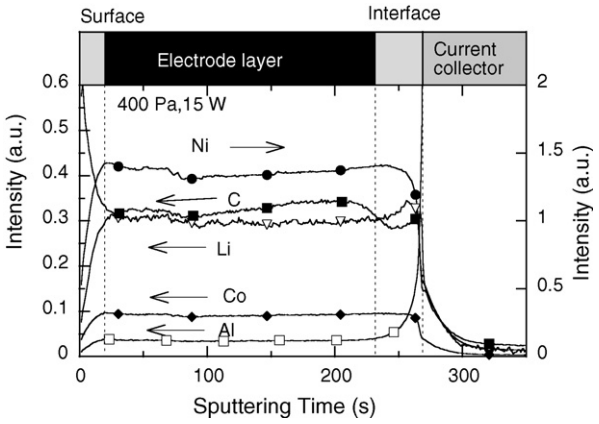

Fig. 2. Variation of optical emission from constituent elements depending on sputtering time in GD-OES measurement of the pristine standard electrode: (■) Ni, (●) Li, (□) C, (▽) Co, and (♦) Al.

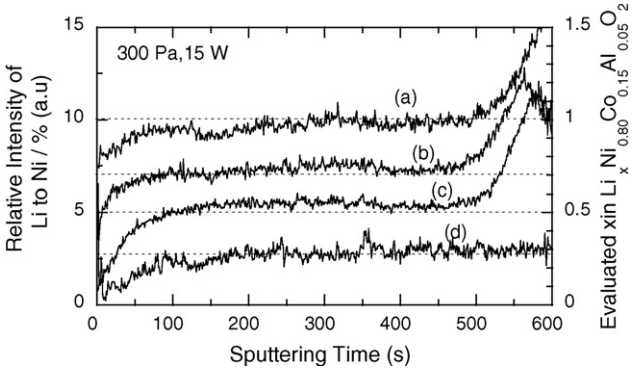

Fig. 3. Variations of relative intensities of emission of lithium to nickel during GD-OES measurement for the positive electrodes of the model cells, and corresponding composition of the active material: (a) pristine electrode, (b) electrode in SOC = 0%, (c) 50%, and (d) 100%.

particles of the active material are spherical where the average size is 7 μm in diameter, and are aggregated by smaller primary particles as shown in Fig. 1b. The result of GD-OES measurement for this electrode is plotted in Fig. 2 where the pressure of Ar atmosphere is 400 Pa and applied power is 20 W. Strong emission is observed from nickel, which is main metal component of the active material. Cobalt and aluminum which are used as substitution elements in the material also show emission with nickel. After about 250 s in sputtering time, rapid increase is observed for emission of aluminum due to beginning of sputter of the Al current collect. Since the thickness of the electrode layer is 30 μm, sputtering rate is about 7 $\mu m\,min^{-1}$. Gradient of emission intensities for all elements at the interface between the electrode layer and the current collector is mainly caused by heterogeneous structure of the interface as shown in Fig. 1a. Since the aluminum foil is dense and hard compared with the electrode layer, sputtering rate changes slower suddenly after start of sputtering of the current collector. However penetration of the elements into region of the current collector can be seen in Fig. 2, this is also concerned to roughness of the interface. Similarly, at the surface of the electrode corresponding to time region within initial several decade seconds, large variation of emission intensities of elements also observed due to roughness of the surface. Preferential sputtering from ridges of the surface during GD-OES analysis was reported by Shimizu et al. [13], owing to local enhancement in electric field. Thus, the surface is smoothed first, and then uniform sputtering of the electrode layer progress until reaching the current collector. Extremely strong intensity of carbon might be originated from acetylene black as the conductive material in the same reason on electric field. During the sputter of the electrode layer from 40 s to 230 s in sputtering time, uniform profiles of emission strength are observed for Ni, Li, Co, and Al, which are constituent elements of the active material. Since the emission strength is proportional to concentration of the element, this result suggests that the particles of active material are dispersed uniformly in the electrode layer. On the while, concentration gradient is observed for C in the region of the electrode layer. While concentration of carbon is higher in deeper region in some samples as shown in Fig. 2, some other samples show reverse profile. Distribution of the PVdF binder and acetylene black may be influenced by preparation condition of electrode.

Depth profiles of lithium analyzed from the results of GE-OES are plotted in Fig. 3 for the positive electrodes after cell construction. The distribution of nickel, which is main transition metal element of the active material, is assumed being uniform in the electrode layer, and relative emission intensity of lithium to nickel was calculated. In electrochemical system of lithium-ion battery, lithium ions are de-intercalated from the positive electrode during charging process, and are intercalated into the electrode during discharging process. The composition of the active material can be described as $Li_xNi_{0.80}Co_{0.15}Al_{0.05}O_2$ in the test cells, and only the value of x varies during cycling depending on SOC. This lithium composition x of the model cells can be evaluated by using the result of the pristine electrode as the standard. In Fig. 3, averaged value of relative intensity in the region of electrode layer for the pristine electrode is correspondent to unity in x, and depth profiles of x in the other electrodes are evaluated under this premise. At the fully charged state (SOC = 100%), x is not 1 due to limitation of voltage and large capacity loss during initial charging. For all samples, uniform distribution of lithium composition in depth direction is confirmed regardless of SOC. The dotted lines in Fig. 3 show x values for each samples measured by ICP measurement, and these are agree with the results of GD-OES. The lithium compositions of sample electrodes were also estimated from integration of all charged and discharged quantities of electricity considering initial total amount of active materials in the cells. The results are summarized in Table 1. Good coincidence of three results proves accuracy of GD-OES analysis. Increase in lithium composition after about 500 s where is interface of the electrode and the current collector in Fig. 3 is not essential. We also attempted GD-OES analysis of the positive electrodes with sputtering in the reverse direction from the interface-side to the surface-side after peeled off the current collector, and the result did not show increasing behavior of lithium at the interface.

Depth profile analysis by GD-OES was also applied to the positive electrodes from the lithium-ion batteries supplied for

Table 1
Lithium composition x in $Li_xNi_{0.80}Co_{0.15}Al_{0.05}$ in the model cells evaluated by several methods

SOC (%)	ICP[a]	Electricity[b]	GD-OES[c]
0	0.70	0.68	0.73
5	0.50	0.48	0.54
100	0.27	0.28	0.27

[a] Results of ICP measurement.
[b] Results from integration of charged and discharged quantities of electricity.
[c] Results of GD-OES.

degradation test in order to examine variation of lithium distribution in degraded electrodes. The cycle test had been carried out at 0 °C, 20 °C, 40 °C, and 60 °C in CRIEPI [11]. After 50,000 cycles, relative capacities of the test cells were 0.96, 0.96, 0.95, and 0.91, respectively for tested temperature, compared with their initial capacities. In the same manner, relative dc resistance faded to 1.16, 1.11, 1.11, and 1.27. As like these results, especially in the result of the test at 60 °C of high temperature, large degradation was occurred. In Fig. 4, the typical results of GD-OES analysis are plotted for the positive electrodes of supplied batteries for the cycle test. The thickness of the electrode layer was 40 μm, and sputtering rate was about 5 μm min^{-1} for these samples in the condition of 350 Pa in pressure and 15 W in power. Both in the non-tested initial samples and in the samples applied the cycle test, distribution of lithium composition in the electrode layer is almost uniform without remarkable gradient. Dependency on the temperature during the test is not also significant.

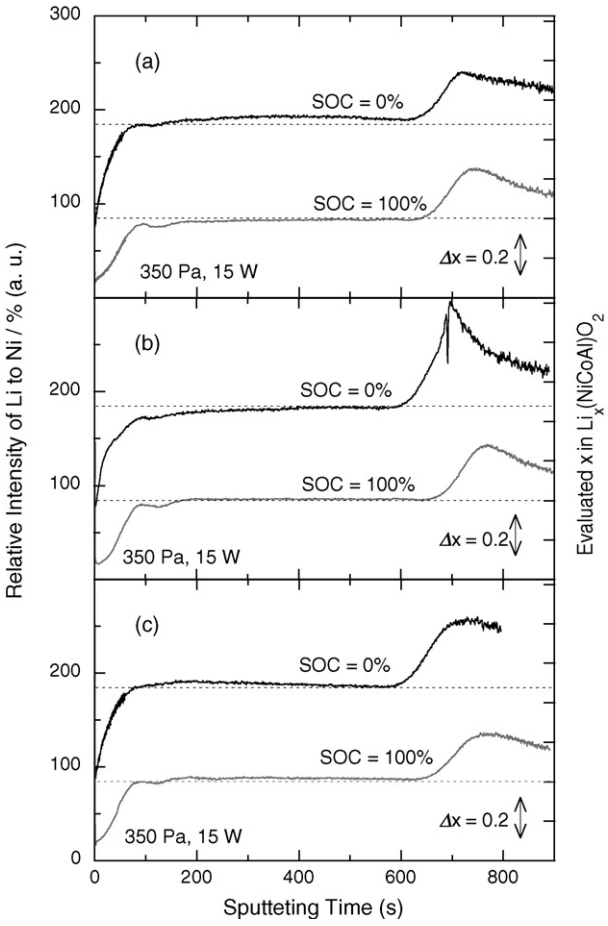

Fig. 4. Depth profiles of lithium normalized by nickel for the positive electrodes in the supplied batteries at SOC = 0% and 100%: (a) non-tested initial samples and (b) tested samples at 0 °C and (c) 60 °C.

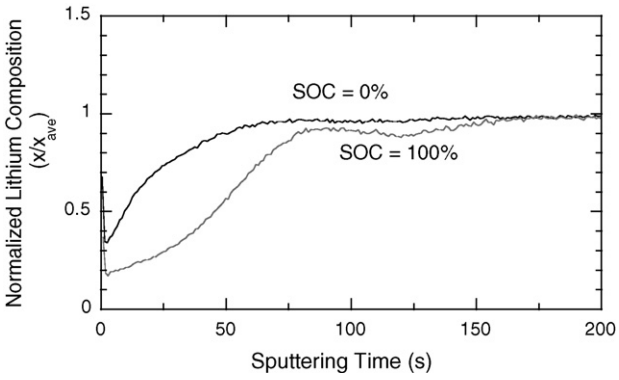

Fig. 5. Normalized relative intensities of lithium to nickel for the positive electrodes in the supplied batteries at SOC = 0% and 100%.

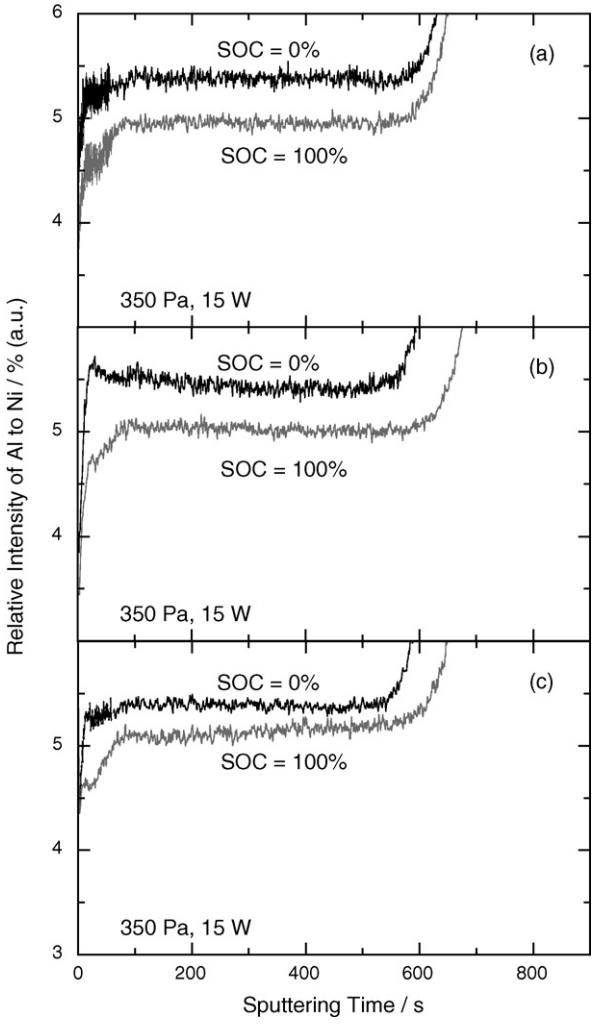

Fig. 6. Depth profiles of aluminum normalized by nickel for the positive electrodes in the supplied batteries at SOC = 0% and 100%: (a) non-tested samples and (b) tested samples at 0 °C and (c) 60 °C.

The profiles of lithium composition in the surface vicinity of the electrode tested at 40 °C are plotted in Fig. 5 where the lithium composition has been normalized to the averaged value between 200 s and 500 s in sputtering time. Gradient portion of the plots is corresponding to particles of the active material located surface of the electrode layer. Comparison of the results of charged and discharged states suggests that lithium concentration at the surface is especially lower than that at the inside of the particles in the discharged state. During charging process of the batteries, lithium ions are de-intercalated from the positive electrode material. Since the de-intercalation occurred from the surface of each particle of the active material, concentration gradient is produced from inside to surface of the particle if diffusion of lithium in the particle is not so fast. On the contrary, lithium concentration at surface becomes higher than inside during discharge. Hence distribution profile shown in Fig. 5 is reasonable. The concentration gradient of lithium formed in the particles is not dissolved completely even after the end of charge as shown in Fig. 5 suggesting slow diffusion of lithium in the particle. Hence, if the lithium composition gradient has been formed in the electrode layer during cycling, it may remain long time. The uniform distribution of lithium in the electrode layer is not produced after the cycle test by lithium diffusion but during the test, and all particles of the active materials in whole electrode layer contribute to electrode reaction homogeneously during cycling in the tested batteries. Thus, it can be concluded that the results of surface analysis using EXAFS [2], XPS [3], FT-IR [4], etc., could be thought to represent characteristics of the whole electrode.

Depth profiles of the elements besides lithium were also analyzed. In the profiles of aluminum, dependency on SOC was observed as shown in Fig. 6. In all electrodes, aluminum composition is slightly larger at SOC = 0% than that at SOC = 100%. Especially large gradient was appeared in the results at SOC = 100% suggesting aluminum deficiency was formed on the surface in charged state. Note that the wavelength selected for aluminum was 396.15 nm was not interfered by emission of lithium. When the positive electrode consisted of lithium nickel oxide-based material without partial substitution of aluminum was analyzed by GD-OES, emission from aluminum was detected only in the region of the current collector. Hence the variation of aluminum composition depending on SOC as shown in Fig. 6 is not related with the current collector. Supporting results were obtained from ICP measurement for the electrodes where 2% of aluminum decreased in the charged state. It is supposed that small amount of aluminum in the active material reacts as like lithium during cycling. Further study is needed to prove the reaction.

Apart from the determination of distributions of the constituent elements in the electrode layers, observation of particles inside the electrodes, which were exposed by sputter in GD-OES, was examined by using SEM. Fig. 7a shows a typical SEM image of the exposed face in the positive electrode where is bottom of crater produced by sputter. The sample shown in Fig. 7a had been applied the cycle test at 40 °C, and SOC was set to 0% after the test. In GD-OES measurement, sputter had been stopped at 200 s, and the depth of the face from the surface corresponded to about 10 μm. It is confirmed that the face is flat and smooth plane, and the particles of active materials show their cross sections. Itoh and Ukyo [14] reported that many cracks were observed at grain boundary in particles of positive

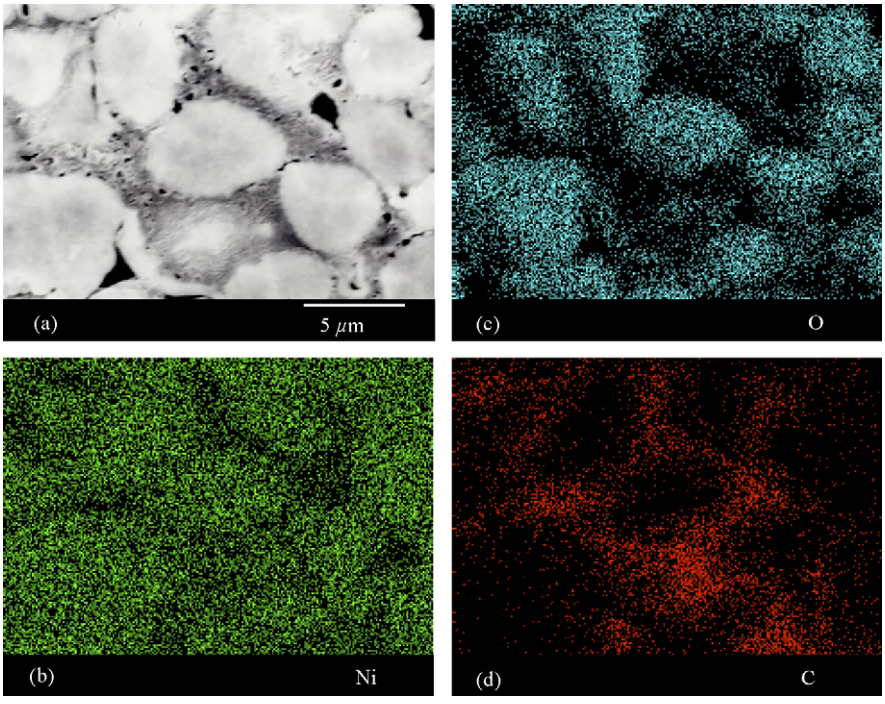

Fig. 7. (a) SEM images of sputtered face (about 10 μm of depth from the surface) by GD-OES inside the positive electrode of a supplied batteries at SOC = 0% after the cycle test at 40 °C and distribution of (b) nickel, (c) oxygen and (d) carbon analyzed by energy dispersive X-ray spectroscopy.

electrode after cycling by using focused ion beam (FIB) technique with SEM, and that the formation of the cracks caused increase of resistance. Dees et al. [15] also mentioned that isolation of finer particles was one of possible sources for interfacial impedance increase in their simulation study on ac impedance. In our electrodes, such cracks or collapses of the particles are not observed remarkably, and these are not decisive factor of degradation. Thus, variation of surface structure of the positive electrode is suggested as the primary factor of increase in interfacial increase (reaction resistance) resulting in power fade of the batteries.

In order to analyze distribution of the elements in the exposed face, energy dispersive X-ray spectroscopy (EDS) was carried out with SEM observation. Fig. 7b–d shows the results of EDS for nickel, oxygen and carbon, respectively. It is confirmed that bright particles in Fig. 7a are nickel oxide-based material, and these are linked each other by thin filmy material containing carbon, that is PVdF binder. Thus, GD-OES combined with SEM–EDS analysis gives important information about structure inside the electrode layer.

4. Conclusions

GD-OES was a convenient method to obtain depth profile of the electrode layer of lithium-ion battery from the surface to the interface with the current collector. In addition, combination of GD-OES with SEM–EDS enabled us the observation of the inside of the electrode layer. For the pristine electrode, while uniform distribution was confirmed for the elements of the active material in the electrode layer, small gradient was observed for carbon, which was main element of the conductive additive, the binder, and the electrolyte solvent. On the degradation of the battery performance such as dc resistance by the applied cycle test, relation with the lithium distribution in the positive electrode layer is not significant. Cracks and collapses were not observed clearly in the particles of the active materials, suggesting they were not main factors of degradation. The results of GD-OES also suggested aluminum composition in $Li_x(NiCoAl)O_2$ changed slightly during charging and discharging.

Acknowledgements

This work was done in the "Development of Lithium Battery Technology for Use by Fuel Cell Vehicles" of New Energy and Industrial Technology Development Organization (NEDO) with financial supports of Ministry of Economy, Trade and Industry (METI) and NEDO. The authors would like to thank Mr. Ozaki of Matsushita Battery Industrial Co. Ltd. for supplying the battery cells used in this research and Dr. Kihira of CRIEPI for providing the cells degraded by the cycle test. For the preparation of the standard electrodes and the model cells, disassembly of the batteries and ICP measurement, Dr. Kobayashi of AIST is gratefully acknowledged.

References

[1] Y. Saito, J. Power Sources 146 (2005) 770–774.
[2] H. Kobayashi, M. Shikano, S. Koike, H. Sakaebe, K. Tatsumi, J. Power Sources 174 (2007) 380.
[3] M. Shikano, H. Kobayashi, S. Koike, H. Sakaebe, E. Ikenaga, K. Kobayashi, K. Tatsumi, J. Power Sources 174 (2007) 795.
[4] M.K. Rahman, S. Saito, J. Power Sources, in press.
[5] M. Doyle, J. Newman, A.S. Gozdz, C.N. Schmulz, J.-M. Tarascon, J. Electrochem. Soc. 143 (1996) 1890–1903.
[6] R.K. Marcus, J.A.C. Broekaert (Eds.), Glow Discharge Plasmas in Analytical Spectroscopy, John Wiley & Sons Ltd., Chichester, 2003.
[7] R. Payling, D. Jones, A. Bengtson (Eds.), Glow Discharge Optical Emission Spectrometry, John Wiley & Sons Ltd., Chichester, 1997.
[8] D. Payling, Spectroscopy 13 (1998) 36–44.
[9] K. Shimizu, H. Habazaki, P. Skeldon, G.E. Thompson, Surf. Interf. Anal. 35 (2003) 564–574.
[10] K. Shimizu, H. Habazaki, P. Skeldon, G.E. Thompson, Spectrochim. Acta B 58 (2003) 1573–1583.
[11] N. Kihira, N. Terada, Proceedings of the 22nd International Battery, Hybrid and Fuel Cell Electric Vehicle Symposium & Exposition, 2006.
[12] N. Kihira, Y. Mita, K. Takei, Y. Kobayashi, H. Miyashiro, K. Kumai, N. Terada, T. Iwahori, Proceedings of the 206th ECS Meeting, 2004, Abstract # 385.
[13] K. Shimizu, H. Habazaki, P. Skeldon, G.E. Thomson, G.C. Wood, Surf. Interf. Anal. 27 (1999) 950–954.
[14] Y. Itoh, Y. Ukyo, J. Power Sources 146 (2005) 39–44.
[15] D. Dees, E. Gunen, D. Abraham, A. Jansen, J. Prakash, J. Electrochem. Soc. 152 (2005) A1409–A1417.